THERMODYNAMICS ANALYSIS OF SOLAR-EJECTOR PUMP OTEC (SEP-OTEC) RANKINE CYCLE USING AMMONIA AS REFRIGERANT

Muhammad Aiman Wafi Suruji[,1], Nik Ridhwan[1,2]*, Nazri Nasir[1,2], Muhammad Ajwad Wahinuddin[1], Norazila Othman[1,2], and Shabudin Mat[1,2]

[1]Faculty of Mechanical Engineering, Universiti Teknologi Malaysia, 81310 UTM Johor Bahru, Johor, Malaysia

[2]UTM Aerolab, Institute of Vehicle System and Engineering (IVeSE), Universiti Teknologi Malaysia, 81310 UTM Johor Bahru, Johor, Malaysia

*Corresponding email: ridhwan@utm.my

ABSTRACT

Organic Rankine Cycle (ORC) applications include ocean thermal energy conversion (OTEC), in which mechanical work is generated from heat energy to rotate generators and generate electricity. The OTEC system heated and cooled its refrigerant by taking advantage of the relatively small temperature difference between the warmer surface seawater and the colder deep seawater. The low-temperature difference between seawater and the rest of the system meant that the thermal efficiency of the system was relatively low; to address this problem, the OTEC cycles needed to be revised. To increase the basic OTEC cycle's thermal efficiency by 3.3–4.0%, various modifications have been developed. Two such cycles are the Solar Boosted OTEC (SOTEC) cycle and the Ejector Pump cycle (EP-OTEC). While the two improvements alter the rotating turbine parameters in different ways, they can be combined to create an improved OTEC cycle through the use of thermodynamics. In this study, an algorithm for revised OTEC was developed using MATLAB, and the performance of the system after the modifications was further quantified. This SEP-OTEC cycle thermal efficiency gives a 1.2-fold improvement when compared to the previous OTEC cycle thermal efficiency, which was 3.1%.

Keywords: OTEC*, Rankine cycle, solar, ejector, ammonia*

1.0   INTRODUCTION

The generation of electricity in Malaysia today is primarily reliant on natural gas as well as coal [1]. Carbon dioxide is a by-product that is created as a result of the use of these primary sources of energy [2]. The by-product may have unintended consequences for the environment, such as contributing to climate change [3]. As a result, Malaysia requires alternative energy sources, also known as renewable energy sources, in order to lessen its reliance on coal and natural gas [4]. It is for the purpose of minimizing the production of greenhouse gases (GHG), as numerous studies have mentioned that GHG has an adverse effect on the environment and shortens the earth's lifespan [5]. It is common knowledge that one of the potential sources of renewable energy in Malaysia is ocean energy, particularly in areas close to the South China Sea [6]. An Organic Rankine Cycle (ORC), also known as the OTEC system, can be used to extract energy from the ocean by taking advantage of the temperature difference between warm surface seawater caused by solar

radiation and cold deep seawater. This temperature difference is mentioned in a number of studies that were conducted in the past [7].

The OTEC system makes use of heat to generate electricity by taking advantage of the difference in temperature that exists between warm seawater and cold seawater [8]. Under the Twelfth Malaysia Plan, Malaysia has recently invested nearly RM 6 million for its first experimental OTEC powerplant [9]. This move is part of the country's efforts to move toward a more sustainable environment. The low-temperature difference of seawater can only achieve a maximum thermal efficiency of 3.1%, according to the research that was reported in [10]. Solar Boosted OTEC (SOTEC) and Ejector Pump OTEC (EP-OTEC) are two examples of the revised OTEC cycles that have been developed and introduced by researchers so far in an effort to improve thermal efficiency [11, 12]. The SOTEC cycle made use of a solar collector to convert solar radiation into heat that was then used to heat the refrigerant in the evaporator [13]. This heat was then directed into the inlet of a turbine to produce power. In contrast, the EP-OTEC cycle generated low pressure at the turbine outlet by utilizing a liquid-vapor ejector that was integrated with a pump as the driving mechanism [14]. This allowed for the generation of power. It is true that SOTEC modifies the parameter of the turbine inlet, but EP-OTEC modifies the parameter of the turbine outlet, which results in a higher level of thermal efficiency (up to 3.3% and 4.0%, respectively) [10, 15].

Ammonia (NH3) has been shown to be one of the best refrigerants for the OTEC cycle in a number of studies due to the fact that it possesses favorable thermophysical properties [16]. Ammonia as a refrigerant improved the OTEC cycle to produce a higher power output compared to other refrigerants at an equivalent mass flow rate, which unquestionably increased the cycle's thermal efficiency [17]. The thermal efficiency of the cycle is a crucial factor in evaluating OTEC systems [18], so it's worth emphasizing here. The improvement of thermal efficiency results in an increase in the net power output while simultaneously resulting in a decrease in the heat load of the heat exchanger, the size of the main component, and the capital cost of building a power station [19]. As a result, a significant amount of research has been carried out in recent years to improve the thermal efficiency of the OTEC cycle through modifications to the cycle, the refrigerant, and the components [20].

In this investigation, the traditional OTEC cycle is rethought as a modified OTEC cycle with combined EP-OTEC and SOTEC characteristics. These characteristics are achieved with the help of additional components, primarily a solar collector and an ejector pump. An algorithm of thermodynamic analysis has been specifically developed for the purpose of calculating the net power output of this modified cycle by using several input parameters such as the temperature of the seawater's surface, the mass flow rate ratio, and the motive pressure ratio. To achieve the ultimate purpose of this research, the thermal efficiency of the modified cycle is quantified through the numerical simulation of thermodynamic analysis.

2.0   SETUP AND METHODOLOGY

Based on the proposed SEP-OTEC cycle, we used a solar collector array and liquid-vapor ejector with its motive pump to improve the thermal efficiency of the conventional OTEC cycle (Fig. 1). After the condenser, we attached a distributor to divide the refrigerant into two streams (see states 7 and 8). The first stream of refrigerant (state 7) passed a pump before reached an evaporator to extract heat from surface seawater, and the refrigerant transformed to saturated gas (state 1-2). After that, this saturated gas absorbed heat from the solar collector and accordingly changes to superheated gas (state 2-3). The superheated gas is then channeled into a turbine before being pulled by the ejector's suction nozzle (state 3-4). Meanwhile, the second stream of the refrigerant (state 8) was streamed into a motive pump, pressurized, and further headed into a primary ejector's nozzle (state 9). This

compressed refrigerant then reduced its pressure after the primary nozzle (Pn) outlet. The low-pressure condition at the Pn outlet induced the low-pressure condition at the secondary nozzle (Sn) outlet, which resulting suction at the turbine outlet (state 4). After that, both Pn and Sn outlets were channeled into an ejector mixing chamber before being discharged through an ejector diffuser at condensation pressure (state M-5). The discharged refrigerant then released heat to cold seawater that passed through the condenser until it reached a saturated liquid state (state 5-6) and finally completed the cycle.

For the model analysis, all the calculations only involved one-dimensional analysis, including the ejector. The ejector model analysis was based on the two-phase ejector (liquid from the pump and vapor from the turbine), and it was assumed as a homogeneous equilibrium [21]. Meanwhile, the mixing part of the ejector used the Constant-Area Mixing (CAM) assumption instead of the Constant-Pressure Mixing (CPM) due to better performance at the optimum suction nozzle pressure [22]. It was considered that the ejector only operated at the subsonic velocity region instead of the supersonic because the motive pressure value was not in the suitable range; thus, converging-diverging nozzle and shockwave calculation was excluded [23]. In this analysis, we assumed the pressure drop in piping, evaporator, and condenser was negligible and considerably minor. On the other note, the heat transfer only occurs in the evaporator, solar collector, and condenser [24]. The refrigerant left the evaporator and condenser as saturated vapor and saturated liquid, respectively [25].
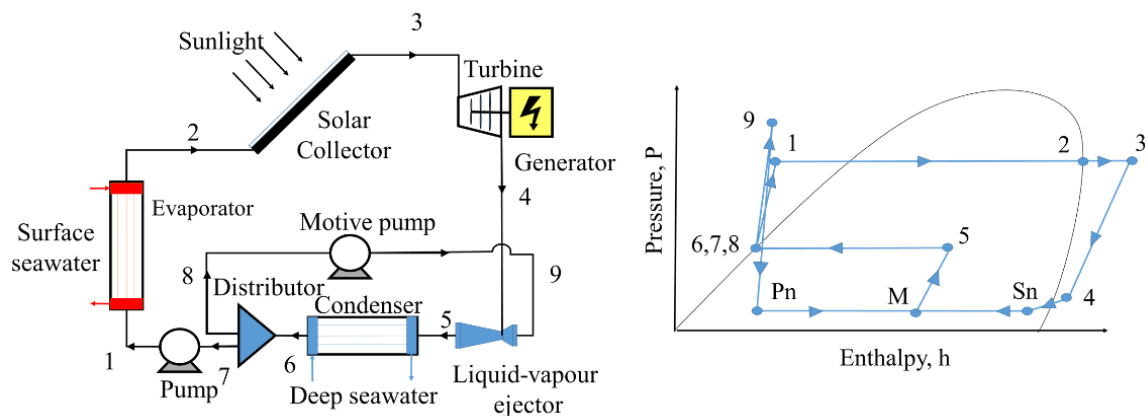

Figure 1: Schematic drawing and pressure-enthalpy (P-h) diagram of the proposed SEP-OTEC.

Table 1: Parameter for the SEP-OTEC cycle.

Parameter	Value	Author
Working fluid	Ammonia (NH_3)	[10]
Gross turbine power	100-200 kW	[15]
Cold seawater	5 – 8 °C	[26]
Seawater temperature difference at the condenser	5.8 °C	[18]
Warm seawater temperature	25.3-31.3 °C	[27]
Seawater temperature difference at the evaporator	3 °C	[18]
Refrigerant temperature at the evaporator outlet	Warm surface seawater -1°C	-
Refrigerant temperature difference at the solar collector	20 - 40 °C	[18]
Turbine efficiency	80% – 85%	[18]
Pump efficiency	65% - 80%	[18]
Primary nozzle efficiency	95%	[28]
Secondary nozzle efficiency	85 %	[28]

Mixer efficiency	95 %	
Diffuser efficiency	85 %	
Mass fraction of motive part	0.3 – 0.9	[18]
Motive pressure ratio	0.8 – 1.3 kPa	

The numerical simulation was carried out in Matlab R2018a using the refrigerant's thermodynamic properties as obtained from CoolProp v6.1.3. At the evaporator's outlet, state 2 was used as the starting point for the calculation. At a temperature 1°C below the surface seawater inlet temperature of the counter-current heat exchanger, the evaporation pressure was the same as the saturation pressure. Equations (1) through (4) were utilized to determine the properties at the evaporator outlet.

$$T_2 = T_{ws,i} - 1 \tag{1}$$
$$P_2 = P(T_2, Q = 1) = P_e \tag{2}$$
$$h_2 = h(T_2, Q = 1) \tag{3}$$
$$s_2 = s(T_2, Q = 1) \tag{4}$$

In accordance with the isobaric process that took place at the output of the solar collector, the pressure was equivalent to the evaporation pressure, and it was then assumed that the temperature would rise by 20 degrees Celsius after that (see equations 5-7 to calculate the other thermodynamic properties).

$$T_3 = T_2 + \Delta T_{sc} \tag{5}$$
$$h_3 = h(T_3, P_2) \tag{6}$$
$$s_3 = s(T_3, P_2) \tag{7}$$

Due to the isobaric nature of the process, it was assumed that the pressure at the main pump outlet was equal to the evaporation pressure and the temperature was 5 degrees Celsius lower than the evaporator outlet temperature. Using equations 8 to 10, the properties of the refrigerant at the evaporator inlet were calculated.

$$T_1 = T_2 - 5 \tag{8}$$
$$h_1 = h(T_1, P_2) \tag{9}$$
$$s_1 = s(T_1, P_2) \tag{10}$$

The motive pressure in the secondary channel was calculated using the equation of motive pressure ratio (see equation 11), and its entropy was equal to the evaporator inlet entropy due to the isentropic process. The main pump outlet's entropy was used as initial data instead of the condenser outlet's entropy (see equation 12 and 13).

$$X_p = \frac{P_m}{P_e} \tag{11}$$
$$h_9 = h(P_m, s_1) \tag{12}$$
$$T_9 = T(P_m, s_1) \tag{13}$$

Given the isentropic process, the pressure and entropy at the ejector's primary nozzle outlet were assumed to be identical to those at the motive pump outlet. The isentropic enthalpy was calculated using equation 14, while the actual enthalpy can be calculated using the primary nozzle efficiency equation (equation 15). Using the mass balance equation and the energy balance equation (equations 16 and 17), an iterative computational process was used to adjust the primary nozzle outlet and then the calculated velocities were compared to ensure the properties obeyed one another (see equation 18-20).

$$h_{pn} = h\left(s_9, P_{pn}\right) \qquad (14)$$

$$\eta_{pn} = \frac{h_9 - h_{pn}}{h_9 - h_{pn,is}} \qquad (15)$$

$$\dot{m}_m = \rho_{pn} A_{pn} V_{pn,mass} \qquad (16)$$

$$h_9 = h_{pn} + \frac{v^2_{pn,energy}}{2} \qquad (17)$$

$$\rho_{pn} = \rho\left(P_{pn}, h_{pn}\right) \qquad (18)$$

$$T_{pn} = T\left(P_{pn}, h_{pn}\right) \qquad (19)$$

$$s_{pn} = s\left(P_{pn}, h_{pn}\right) \qquad (20)$$

Assuming a suction pressure at the turbine's outlet, the actual enthalpy can be calculated using equations 21 and 22, and the other thermodynamic properties using equations 23 and 24.

$$h_{4,is} = h(P_4, s_3) \qquad (21)$$

$$\eta_T = \frac{h_3 - h_4}{h_3 - h_{4,is}} \qquad (22)$$

$$T_4 = T(P_4, h_4) \qquad (23)$$

$$s_4 = s(P_4, h_4) \qquad (24)$$

Equations 25 and 26 were used to figure out the real enthalpy of the secondary nozzle outlet. The energy balance equation and the mass balance equation were used to compare the calculated speeds by changing the pressure at the turbine outlet (equations 27 and 28). Equations 29 and 30 can be used to figure out the other thermodynamic properties.

$$h_{sn,is} = h(P_{pn}, s_3) \qquad (25)$$

$$\eta_{sn} = \frac{h_4 - h_{sn}}{h_4 - h_{sn,is}} \qquad (26)$$

$$h_s = h_{sn} + \frac{v^2_{sn,energy}}{2} \qquad (27)$$

$$m_e = \rho_{sn} A_{sn} V_{sn,mass} \qquad (28)$$

$$\rho_{sn} = \rho\left(P_{pn}, h_{sn}\right) \qquad (29)$$

$$T_{sn} = T\left(P_{pn}, h_{sn}\right) \qquad (30)$$

The mixing pressure was assumed when calculating the velocity at the ejector's mixer outlet using the momentum equation (equation 31). Then the calculated velocity to determine the actual enthalpy of the mixer using equation 32. In addition, the mass balance equation (equation 33) was utilized to calculate the velocity, which was then compared to the velocity derived from the momentum equation. Iterative processes were carried out by varying the mixing pressure until the convergence criteria were met. Equations 34-36 can be used to compute the other thermodynamic properties under the mixing pressure.

$$\eta_{mix}\left(\dot{m}_{mix}V_{pn} + m_e V_{sn}\right) + P_{pn}A_{pn} + P_{sn} = \dot{m}_{total}V_{mix,momentum} + P_{mix}A_{mix} \qquad (31)$$

$$\dot{m}_{pn}\left(h_{pn} + \frac{v^2_{pn}}{2}\right) + \dot{m}_{sn}\left(h_{sn} + \frac{v^2_{sn}}{2}\right) = \dot{m}_{total}\left(h_{mix} + \frac{v^2_{mix,momentum}}{2}\right) \qquad (32)$$

$$\dot{m}_{total} = \rho_{mix}A_{mix}V_{mix,mass} \qquad (33)$$

$$\rho_{mix} = \rho(P_{mix}, h_{mix}) \qquad (34)$$

$$T_{mix} = T(P_{mix}, h_{mix}) \qquad (35)$$

$$s_{mix} = s(P_{mix}, h_{mix}) \qquad (36)$$

The entropy of the diffuser outlet at the ejector was equal to the mixer entropy, and its actual enthalpy was obtained using the energy equation (equation 37). We also calculated

other thermodynamic properties, including the isentropic enthalpy, and the efficiency, using equations 38-40.

$$h_m + \frac{v^2_{mix,mass}}{2} = h_d \tag{37}$$

$$\eta_d = \frac{h_{d,is} - h_m}{h_d - h_m} \tag{38}$$

$$P_d = P(h_{d,is}, S_m) \tag{39}$$

$$T_d = T(h_{d,is}, S_m) \tag{40}$$

Considering the isobaric process, the condenser pressure outlet was equal to the diffuser outlet pressure, and the refrigerant's state was saturated liquid. The other thermodynamic properties can be calculated using equations 41-43.

$$T_c = T(P_d, Q = 0) \tag{41}$$

$$h_c = h(P_d, Q = 0) \tag{42}$$

$$s_c = s(P_d, Q = 0) \tag{43}$$

By considering the isentropic efficiency, computational recalculation at the main pump was required using equations 44-46. The entropy value can be considered equivalent to the entropy of the condenser outlet.

$$h_{1,is} = h(P_e, s_c) \tag{44}$$

$$\eta_p = \frac{h_{1,is} - h_c}{h_1 - h_c} \tag{45}$$

$$T_1 = T(P_e, h_1) \tag{46}$$

On the other note, the motive pump also required recalculation, which considering isentropic efficiency. Besides, the entropy was equal to the entropy of the condenser outlet, and other properties can be calculated with the following equation 47-49.

$$h_{9,is} = h(P_m, S_c) \tag{47}$$

$$\eta_p = \frac{h_{9,is} - h_c}{h_9 - h_c} \tag{48}$$

$$T_1 = T(P_m, h_9) \tag{49}$$

After the recalculation procedure, we used this value to revise the value of the primary nozzle to the condenser outlet until the new entropy of the condenser outlet was obtained. We compared this new entropy value with the entropy of the main pump outlet, then executed the iteration by adjusting the inlet temperature of the evaporator assumed earlier (See fig. 2 for the calculation flowchart). To quantify the overall performance of the cycle, including thermal efficiency and pressure drop ratio as shown in equations 50-58.
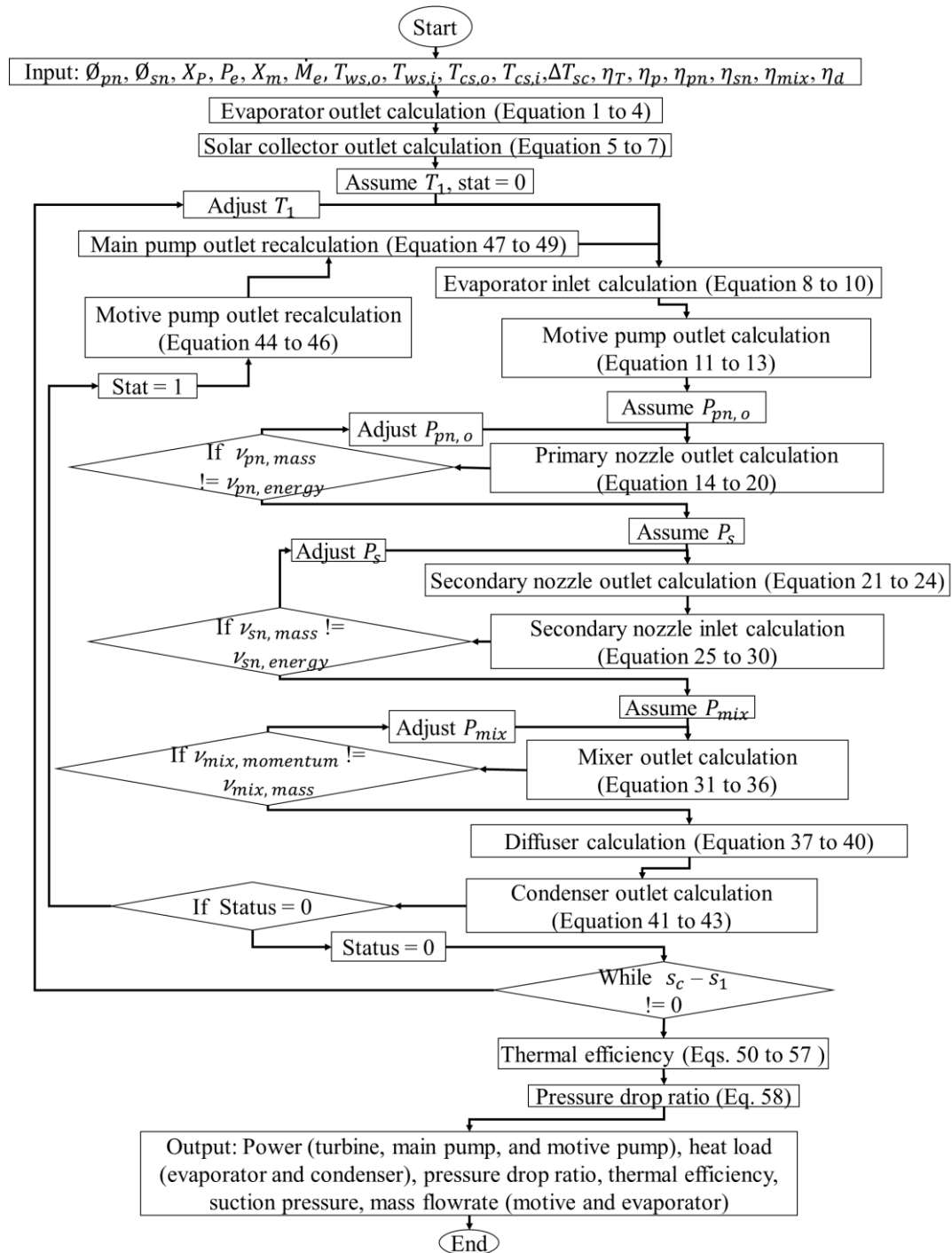
Figure 2: Flowchart of SEP-OTEC Cycle Calculation

For the cycle analysis, data such as thermal efficiency [equation 50-57], pressure drop ratio [equation 58], suction pressure was collected by varying the motive pressure ratio, mass fraction of motive, and the surface seawater temperature.

$$\dot{W}_{turbine} = \dot{m}_e(h_3 - h_4) \qquad (50)$$
$$\dot{W}_{mainpump} = \dot{m}_e(h_1 - h_c) \qquad (51)$$
$$\dot{W}_{motivepump} = \dot{m}_m(h_9 - h_c) \qquad (52)$$

$$\dot{W}_{totalpump} = \dot{W}_{mainpump} + \dot{W}_{motivepump} \qquad (53)$$

$$\dot{Q}_e = \dot{m}_e(h_2 - h_1) \qquad (54)$$

$$\dot{Q}_{sc} = \dot{m}_e(h_3 - h_2) \qquad (55)$$

$$\dot{Q}_{in,total} = \dot{Q}_e + \dot{Q}_{sc} \qquad (56)$$

$$\eta_{th} = \frac{\dot{W}_{turbine} - \dot{W}_{totalpump}}{\dot{Q}_{in,total}} \times 100 \qquad (57)$$

$$\gamma = \frac{P_d - P_4}{P_d} \qquad (58)$$

3.0   RESULTS AND DISCUSSION

Several manipulated thermodynamic parameters of the proposed revised SEP-OTEC cycle, including surface seawater temperature, motive pressure ratio, and motive mass fraction, were assessed. The hot surface seawater (between 25.3 and 31.3 ºC) was directed to the evaporator water inlet, heating up the refrigerant that passed through. The other variable, such as motive's mass fraction, was fixed at 0.28, while its pressure ratio was fixed at 1.2. In many research, it is noted that the motive pressure depended on the surface seawater temperature because the evaporator outlet temperature was always in the range of 1ºC below the surface seawater temperature, and the mass flow rate of the evaporator was fixed at 2.4 kgs^{-1}. The analysis shows that the proposed SEP-OTEC cycle's net turbine power and thermal efficiency were linearly related to the increase in seawater temperature from 25.3 to 31.3 ºC (for thermal efficiency y = 0.26 x 1.46 with norm residual 0.0294, for turbine net power y = 5.78 x 34.51 with norm residual of 0.5970, see Fig. 3). Previous research also obtain the same relation but with different gradient due to the existing of solar collector, different refrigerant used, and different ejector's geometry parameter [18].
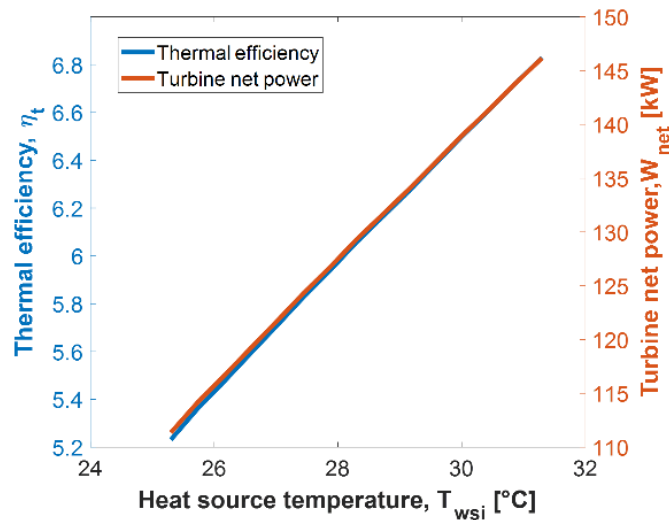

Figure 3: Net turbine power and thermal efficiency of the proposed cycle at different seawater temperatures.

On the other note, the turbine power increase due to the increment of the enthalpy changes in the turbine; likewise, the thermal efficiency also grows because of its linear relationship to the turbine power. It's also worth noting that as the mass fraction of the motive changes, so do the suction pressure, turbine power, pump power, pressure drop ratio, and thermal efficiency of the system. For instance, the suction pressure gradually decreases

as the mass fraction of motive rises, reaching a minimum value of 435.6 kPa at a mass fraction of motive value of 0.1671 (Fig. 4A). The motive pump's suction pressure, however, recovers and increases once more as a result of the increased suction nozzle outlet density.

Meanwhile, as the motive pump's mass fraction rises, the pressure drop ratio does too ($4692x^2 + 1964.4x$ 183.5 with a norm of residual of 0.3734, Fig. 4C), underscoring the significance of the ejector in boosting refrigerant velocity in the tubing and causing the pressure drop at the primary nozzle outlet. Additionally, at a mass fraction of motive value of 0.1536, the revised cycle's thermal efficiency reaches a peak value of 6.83%. (Fig. 4D). The maximum value of thermal efficiency and the trend of its changes, however, do not match the maximum value of turbine power. Due to the decrease in pressure drop ratio, low total pump power, and decreased evaporation capacity ($12307x^2+2797.2x$ 1902.6 with a norm of residual of 1.5899, Fig. 4C), this misalignment occurs. At the area with the highest turbine power, it is clear that an increase in turbine power does not result in an increase in total pump power; instead, a decrease in efficiency is caused by a reduction in evaporation capacity.

As the motive pressure ratio rises and total pump power decreases, the thermal efficiency of the revised SEP-OTEC cycle increases (0.5 to 0.6, Fig. 5A). When the motive pressure ratio was 0.68, the proposed cycle's efficiency peaked at 6.8%; however, as the gradient of the pump power began to decline ($4.971015e-223.6x + 26.89e-5.24x$ with an adjusted R-square of 0.9127), the efficiency gradually decreased ($y=-9582x+7.49$ with an adjusted R-square of 0.9955) due to the decline in gross turbine power ($-26.75x+181.85$ with a norm of residual (Fig. 5B). It should be noted that when the ideal motive pressure ratio and ideal mass fraction of the used motive are 0.68 and 0.1536, respectively, he maximum thermal efficiency can be achieved (Fig. 5A).
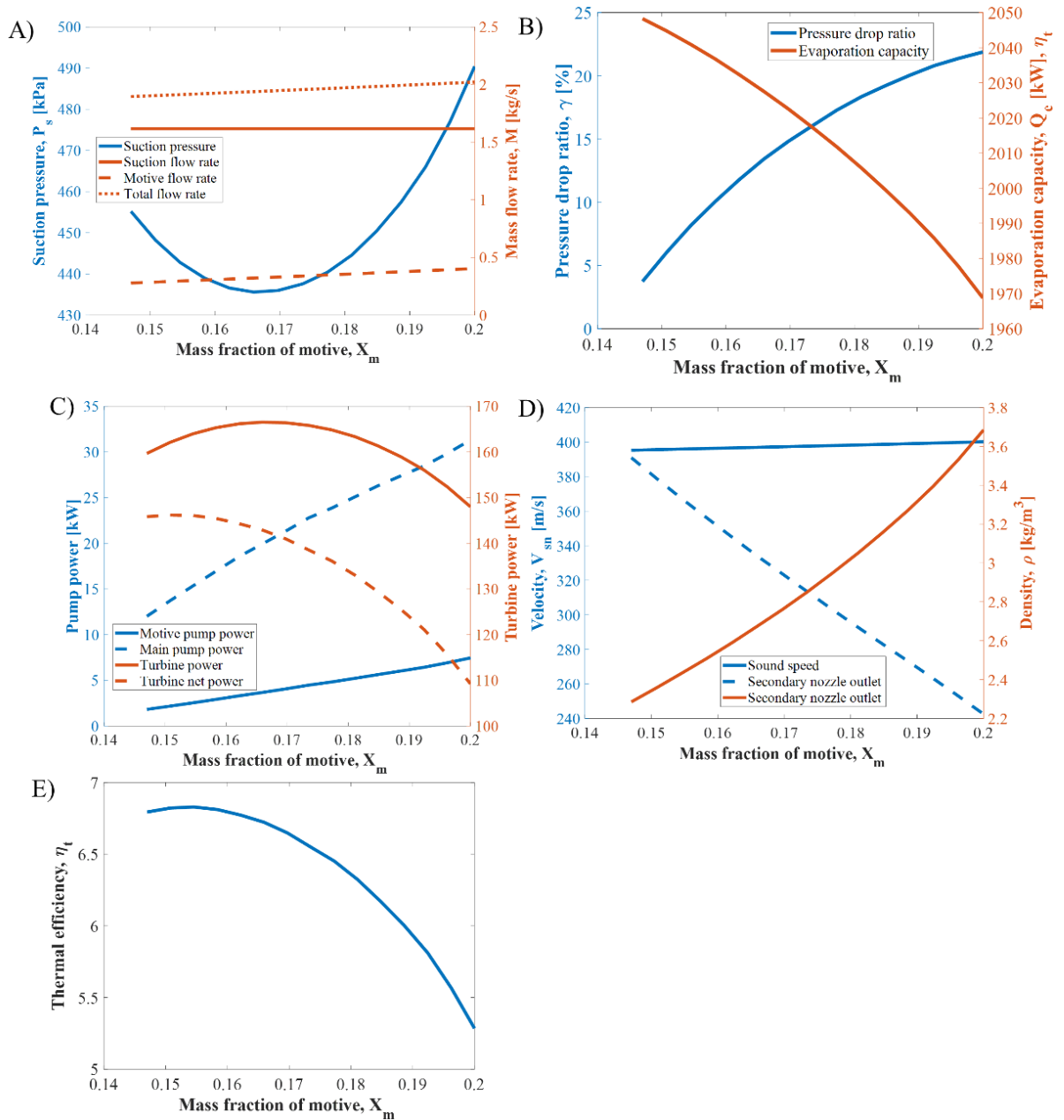
Figure 4: The relationship of thermodynamic performance with various ranges of a mass fraction of motive.

As a conclusion, this SEP-OTEC cycle thermal efficiency results in an improvement of 1.2 times over the previous traditional OTEC cycle thermal efficiency of 3.1%. Further comparing the individual SOTEC and EP-OTEC cycles reveals that the improvements are only about 106% and 70%, respectively [11, see Table 1].
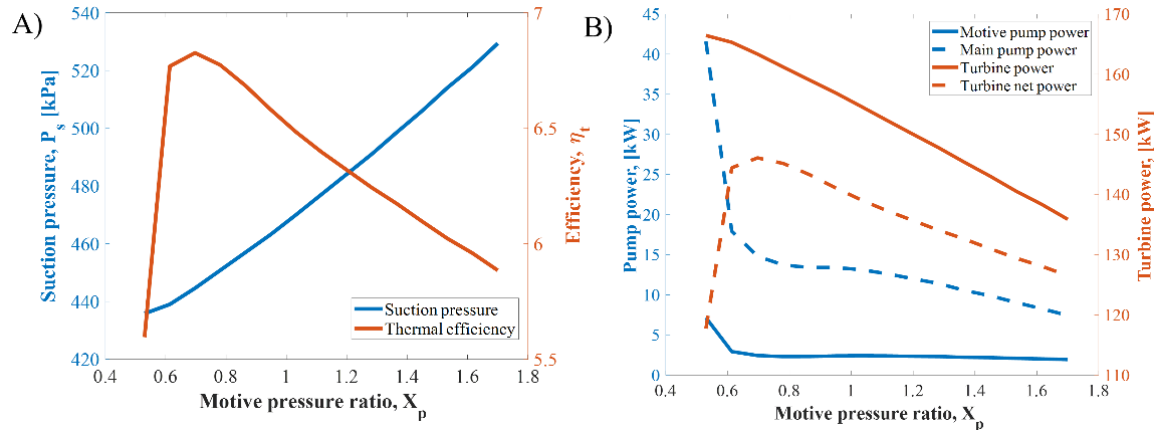
Figure 5: The relationship of suction pressure, pump, and turbine power with various ranges of a mass fraction of motive.

4.0 CONCLUSION

The purpose of the present study is to determine the thermal efficiency of ORC by adding the solar collector into the EP-OTEC system and demonstrate the significance of developing a SEP-OTEC system, which combines an ejector pump and solar energy, as an improvement to the conventional OTEC system. Matlab and Coolprop were used to develop a computer programme that solved the numerical simulation. According to the study, the 3.1% thermal efficiency of the traditional OTEC cycle is improved by 1.2 times by using the SEP-OTEC cycle. Further comparison of the individual SOTEC and EP-OTEC cycles reveals that the improvements are about 106% and 70%, respectively. This study is highly recommended to help the OTEC system to generate the renewable energy to electrical energy. Establishing the methodology can help the OTEC system increase the thermal efficiency and reduce the dependency to the conventional fuel to generate electricity in the future.

ACKNOWLEDGMENTS

NOMENCLATURE

$\varnothing$	Diameter (m)
A	Cross-sectional area (m^2)
$\dot{m}$	Mass flowrate ($kg \cdot s^{-1}$)
P	Pressure (kPa)
Q	Vapour quality
s	Entropy ($kJ \cdot kg^{-1} \cdot K^{-1}$)
h	Enthalpy ($kJ \cdot kg^{-1}$)
Xm	Mass fraction of motive
Xp	Motive pressure ratio
V	Volume (m^3)

Greek symbols

γ	pressure drop ratio (ratio between suction pressure and condenser)	
η	Efficiency	
v	Velocity ($m \cdot s^{-1}$)	
ρ	Density ($kg \cdot m^{-3}$)	

Subscripts

c	Condenser
d	Diffuser
e	Evaporator
i	Inlet
is	Isentropic
m	Motive
mix	Mixer
o	Outlet
p	Pump
pn	Primary nozzle
sc	Cold seawater
sn	Secondary nozzle
sw	Warm seawater
t	Turbine
th	Thermal

REFERENCES

1. Abdullah, W.S.W., M. Osman, M.Z.A. Ab Kadir, and R. Verayiah, *The Potential and Status of Renewable Energy Development in Malaysia.* Energies, 2019. **12**(12): p. 2437.
2. Aleksandrowicz, L., R. Green, E.J.M. Joy, P. Smith, and A. Haines, *The Impacts of Dietary Change on Greenhouse Gas Emissions, Land Use, Water Use, and Health: A Systematic Review.* PLOS ONE, 2016. **11**(11): p. e0165797.
3. Huzaifi, M., A. Budiyanto, and J. Sirait, *Study on the Carbon Emission Evaluation in a Container Port Based on Energy Consumption Data.* Evergreen, 2020. **7**: p. 97-103.
4. Susskind, L., J. Chun, S. Goldberg, J.A. Gordon, G. Smith, and Y. Zaerpoor, *Breaking Out of Carbon Lock-In: Malaysia's Path to Decarbonization.* Frontiers in Built Environment, 2020. **6**(21).
5. Syafrudin, s., M. Budihardjo, N. Yuliastuti, and B. Ramadan, *Assessment of Greenhouse Gases Emission from Integrated Solid Waste Management in Semarang City, Central Java, Indonesia.* Evergreen, 2021. **8**: p. 23-35.
6. Jaafar, A.B., *Future Energy: Is OTEC the Solution*, in *myForesight*. 2015. p. 4-5.
7. Muslim, M., M.I. Alhamid, Nasruddin, and B. Ismoyo, *Analysis of the scroll compressor changing into an expander for small scale power plants using an organic rankine cycle system.* Evergreen, 2020. **7**(4): p. 615-620.
8. Sharma, M. and R. Dev, *Review and Preliminary Analysis of Organic Rankine Cycle based on Turbine Inlet Temperature.* Evergreen, 2018. **5**.
9. Jaafar, A.B., M.K. Abu Husain, and A. Ariffin, *Research and Development Activities of Ocean Thermal Energy-Driven Development in Malaysia*. 2020.
10. 1Liu, W., X. Xu, F. Chen, Y. Liu, S. Li, L. Liu, and Y. Chen, *A review of research on the closed thermodynamic cycles of ocean thermal energy conversion.* Renewable and Sustainable Energy Reviews, 2020. **119**: p. 109581.
11. Yoon, J.-I., C.-H. Son, S.-M. Baek, B.H. Ye, H.-J. Kim, and H.-S. Lee, *Performance characteristics of a high-efficiency R717 OTEC power cycle.* Applied Thermal Engineering, 2014. **72**(2): p. 304-308.
12. Yuan, H., P. Zhou, and N. Mei, *Performance analysis of a solar-assisted OTEC cycle for power generation and fishery cold storage refrigeration.* Applied Thermal Engineering, 2015. **90**: p. 809-819.
13. Tewari, K. and R. Dev, *Analysis of Modified Solar Water Heating System Made of Transparent Tubes & Insulated Metal Absorber.* Evergreen, 2018. **5**: p. 62-72.
14. Yoon, J.-I., C. Son, Y. Kim, B. Ye, S. Ha, H.-S. Lee, and H.-J. Kim. *The performance comparison of vapor-vapor ejector OTEC system using wet refrigerants*. 2014.
15. Yamada, N., A. Hoshi, and Y. Ikegami, *Performance simulation of solar-boosted ocean thermal energy conversion plant.* Renewable Energy, 2009. **34**: p. 1752-1758.
16. Samsuri, N., s.a.z. shaikh salim, M. Musa, and M.S. Mat Ali, *Modelling performance of ocean-thermal*

energy conversion cycle according to different working fluids. Jurnal Teknologi, 2016. **78**.

17. Yoon, J.I., C.H. Son, S.M. Baek, H.J. Kim, and H.S. Lee, *Efficiency comparison of subcritical OTEC power cycle using various working fluids.* Heat and Mass Transfer/Waerme- und Stoffuebertragung, 2014. **50**(7): p. 985-996.

18. Yoon, J.-I., S.-H. Seol, C.-H. Son, S.-H. Jung, Y.-B. Kim, H.-S. Lee, H.-J. Kim, and J.-H. Moon, *Analysis of the high-efficiency EP-OTEC cycle using R152a.* Renewable Energy, 2017. **105**: p. 366-373.

19. Caldiño Herrera, U., J.C. García, F.Z. Sierra-Espinosa, J.A. Rodríguez, O.A. Jaramillo, O. De Santiago, and S. Tilvaldiev, *Enhanced thermal efficiency organic Rankine cycle for renewable power generation.* Applied Thermal Engineering, 2021. **189**: p. 116706.

20. Yoon, J.-I., C.-H. Son, S.-H. Seol, C.-M. Son, H.-S. Lee, and H.-J. Kim. *OTEC Cycle Applying a Liquid-vapor Ejector and Motive Pump*. in *The Twenty-fifth International Ocean and Polar Engineering Conference*. 2015.

21. Arsana, M.E., I.G.B. Wijaya Kusuma, M. Sucipta, and I.N. Suamir, *Thermodynamic Analysis of Two-Phase Ejector as Expansion Device with Dual Evaporator Temperatures on Split Type Air Conditioning Systems.* IOP Conference Series: Materials Science and Engineering, 2019. **494**: p. 012034.

22. Atmaca, A., A. Erek, and O. Ekren, *Impact of the mixing theories on the performance of ejector expansion refrigeration cycles for environmentally-friendly refrigerants.* International Journal of Refrigeration, 2018. **97**.

23. Atmaca, A.U., A. Erek, and O. Ekren, *Preliminary Design of the Two-Phase Ejector under Constant Area Mixing Assumption for 5 kW Experimental System.* E3S Web Conf., 2019. **103**: p. 01002.

24. Eldred, M.P., J.C.V. Ryzin, S. Rizea, I.C. Chen, R. Loudon, N.J. Nagurny, S. Maurer, E. Jansen, A. Plumb, M.R. Eller, and V.R.R. Brown. *Heat exchanger development for Ocean Thermal Energy Conversion*. in *OCEANS'11 MTS/IEEE KONA*. 2011.

25. Lecompte, S., H. Huisseune, M. van den Broek, B. Vanslambrouck, and M. De Paepe, *Review of organic Rankine cycle (ORC) architectures for waste heat recovery.* Renewable and Sustainable Energy Reviews, 2015. **47**: p. 448-461.

26. Thiru, S., *Estimation of Ocean Thermal Energy Conversion Resources in the East of Malaysia.* Journal of Marine Science and Engineering, 2020. **9**.

27. Temperatures, G.S., 2021. *Bandar Labuan WATER Temperature: Malaysia: Sea temperatures*. Available from: https://www.seatemperature.org/asia/malaysia/bandar-labuan.htm, [Accessed 17 August 2021].

28. Ma, Z., H. Bao, and A.P. Roskilly, *Thermodynamic modelling and parameter determination of ejector for ejection refrigeration systems.* International Journal of Refrigeration, 2017. **75**: p. 117-128.